Amplification of Seismic Ground Motion in the Fort St. John–Dawson Creek Area, Northeastern British Columbia (NTS 093P, 094A)

P.A. Monahan, Monahan Petroleum Consulting, Victoria, British Columbia, pmonahan@shaw.ca

B.J. Hayes, Petrel Robertson Consulting Ltd., Calgary, Alberta

M. Perra, Petrel Robertson Consulting Ltd., Calgary, Alberta

Y. Mykula, Petrel Robertson Consulting Ltd., Calgary, Alberta

J. Clarke, Petrel Robertson Consulting Ltd., Calgary, Alberta

B. Galambos, Frontier Geosciences Inc., North Vancouver, British Columbia

D. Griffiths, Frontier Geosciences Inc., North Vancouver, British Columbia

O. Bayarsaikhan, Frontier Geosciences Inc., North Vancouver, British Columbia

U. Oki, Northern Geo Testing and Engineering, Fort St. John, British Columbia

Monahan, P.A., Hayes, B.J., Perra, M., Mykula, Y., Clarke, J., Galambos, B., Griffiths, D., Bayarsaikhan, O. and Oki, U. (2020): Amplification of seismic ground motion in the Fort St. John–Dawson Creek area, northeastern British Columbia (NTS 093P, 094A); *in* Geoscience BC Summary of Activities 2019: Energy and Water, Geoscience BC, Report 2020-02, p. 1–12.

Introduction

Seismicity in northeastern British Columbia (BC) has increased significantly recently due to hydraulic fracturing and water disposal by the petroleum industry (Atkinson et al., 2016; Kao et al., 2018). Most of these events are small, but rare events up to magnitude (M) 4.6 have occurred (Babaie Mahani et al., 2017a, b, 2019). Ground motions for the largest of these events are at the lower bound of possible damage, in the range of modified Mercalli intensity (MMI) VI (Worden et al., 2012; Babaie Mahani and Kao, 2018; Babaie Mahani et al., 2019), and minor damage has been reported or is suspected. These events occur at very shallow depths, 1 to 3 km, and partly because of this, events as low as M 0.8 have been felt by residents of the region.

Monahan et al. (2019) recently completed a regional assessment of the potential for amplification of seismic ground motions due to local differences in near-surface geological materials in the Montney play area, currently the most active oil and gas play in BC. Their mapping was based on existing surficial geological maps, generally at a scale of 1:250 000 (e.g., Mathews, 1978; Reimchen, 1980), and they noted a number of inconsistencies between amplifications from instrumentally recorded events and those predicted by the mapping. Consequently, a follow-up study was initiated in the Fort St. John–Dawson Creek area, which is the most heavily populated part of the Montney play area, and where a M 4.6 event occurred in November 2018 (Babaie Mahani et al., 2019). The objectives of this study are to refine the surficial geological mapping, generate a map more representative of shallow subsurface conditions by collecting additional subsurface geological data, and obtain additional shear-wave velocity (V_S) data to better understand the distribution of geological materials susceptible to amplification. The new mapping will be done at a scale of 1:100 000. The purpose of this paper is to present some of the initial results of this investigation: surface geological investigations, subsurface geological data acquisition, the summary of newly acquired V_S data, and interviews with residents who have experienced frequent seismic events.

Ground-Motion Amplification

Ground-motion amplification due to shallow geological conditions can be estimated by the average V_S in the upper 30 m (V_{S30}; Kramer, 1996; Finn and Wightman, 2003). The National Earthquake Hazards Reduction Program (NEHRP) in the United States has defined five Site classes (A to E) based on V_{S30} and these have been adopted by the National Building Code of Canada (Table 1; Building Seismic Safety Council, 2003; National Research Council, 2015).

The V_{S30} is the time-averaged V_S in the upper 30 m (i.e., harmonic mean) and is calculated using the following formula:

$$V_{S30} = \Sigma h / \Sigma t$$

---

where h = each measured interval thickness, where Σh = 30 m, and t = the measured interval travel time; $t = h/V_S$ for each interval.

Moderate to high amplification of seismic ground motions can occur in Site classes D and E.

Amplification can also be due to resonance, where the dominant period of the ground motions is the same as the dominant site period. The dominant site period (T) is calculated by the quarter wavelength rule (Kramer, 1996; Finn and Wightman, 2003):

$$T = 4H/V_S$$

where H = thickness of the low velocity layer, and V_S = the average shear-wave velocity of the low velocity layer.

Amplification due to resonance was also suspected in the region by Monahan et al. (2019).

Regional Geology

The project area extends from Fort St. John to Dawson Creek and from the Alberta border west to the Pine and Moberly rivers (Figure 1), in the western part of the Alberta Plateau (Holland, 1976). Hilltops in the western part are up to 900 m in elevation, with up to 200 m of local relief, and the topography becomes more subdued toward the east, where hilltops are up to 700 m in elevation and local relief is 50 m. The <250 m deep valleys of the Peace River and its major tributaries, the Kiskatinaw, Pine, Moberly and Beatton rivers, are the result of the incision by the rivers into this plateau surface.

Bedrock consists of gently easterly dipping, relatively soft Cretaceous sedimentary rocks (Irish, 1958; Stott, 1982; McMechan, 1994). The principal geological units exposed from northwest to southeast across the project area are, in ascending order: the Shaftesbury Formation, which consists of marine shale; the Dunvegan Formation, which consists of interbedded sandstone, conglomerate and shale; the Kaskapau Formation, which consists of marine shale; and the Cardium Formation, which consists of interbedded sandstone, conglomerate and shale. The upper 10 to 20 m of bedrock is commonly weathered to clay, particularly the shale intervals, and the upper surface is commonly observed to be glaciotectonized in outcrop (e.g., Monahan et al., 2019).

At least three glaciations occurred during the Quaternary in this area (Mathews, 1978; Hartman and Clague, 2008; Hickin et al., 2016a). Deposits of the last two glacial and adjoining nonglacial periods show a repetitive pattern of fluvial incision and deposition during nonglacial intervals, followed by deposition of glaciolacustrine silt as drainageways were blocked by advancing Laurentide ice, and finally, by till during the glacial maximum. Fluvial incision cut deeper following each glaciation, so that modern valleys of the Peace River and its major tributaries are incised through the older Quaternary deposits into bedrock.

Deposits of the latest glaciation, which is Late Wisconsinan in age, are the best known. Both Cordilleran and Laurentide ice extended into the area, but the maximum extents of each appear to have been out of sync. West of the project area, Cordilleran till has been reported interbedded with advance-phase glaciolacustrine deposits (Hartman et al., 2018). The advance-phase glaciolacustrine deposits are overlain by clay-rich and clast-poor till deposited by Laurentide ice. The ice sheets appear to have coalesced, but in the latter stages, the Laurentide till appears to have been overridden by Cordilleran ice (Hickin et al., 2015). As Laurentide ice retreated, drainage was again blocked, resulting in widespread deposition of glaciolacustrine silt, clay, and very fine sand in glacial Lake Peace (Mathews, 1978, 1980; Hartman and Clague, 2008; Hickin et al., 2016a, b).

Sediments older than the last glacial maximum are restricted to Quaternary river valleys (paleovalleys) and are exposed only in the valley walls of the Peace River and other major rivers. Elsewhere, only till and retreat-phase deposits of the most recent glaciation and Holocene sediments can be mapped at the surface. Surficial units have characteristic geomorphic expressions (Mathews, 1978; Hartman and Clague, 2008; Hickin et al., 2015; Monahan et al., 2019). Rolling uplands are underlain mainly by clay till with a veneer of glaciolacustrine silt and clay. Topography in the upland areas is largely controlled by bedrock, which is locally exposed and generally within a few metres of the surface in the western parts of the project area. However, in the upland areas of more subdued relief in the eastern part of the project area, till forms a blanket locally up to 30 m thick. Low relief platforms and terraces, between the uplands and deeply incised major valleys, are underlain by retreat-phase glaciolacustrine and related deposits. Terraces on the walls of major valleys are underlain by late stage gla-

Table 1. National Earthquake Hazards Reduction Program (NEHRP) Site classes (Building Seismic Safety Council, 2003). Susceptibility ratings from Hollingshead and Watts (1994).

Site Class	General description	Definition by V_{S30} (m/s)
A	Hard rock	$V_{S30}>1500$
B	Rock	$760<V_{S30}<1500$
C	Very dense soils and soft rock	$360<V_{S30}<760$
D	Stiff soils	$180<V_{S30}<360$
E	Soft soils, or soil profile with >3 m soft silt or clay	$V_{S30}<180$, or >3 m silt and clay with plasticity index >20, moisture content >40%, and undrained shear strength <25 kPa

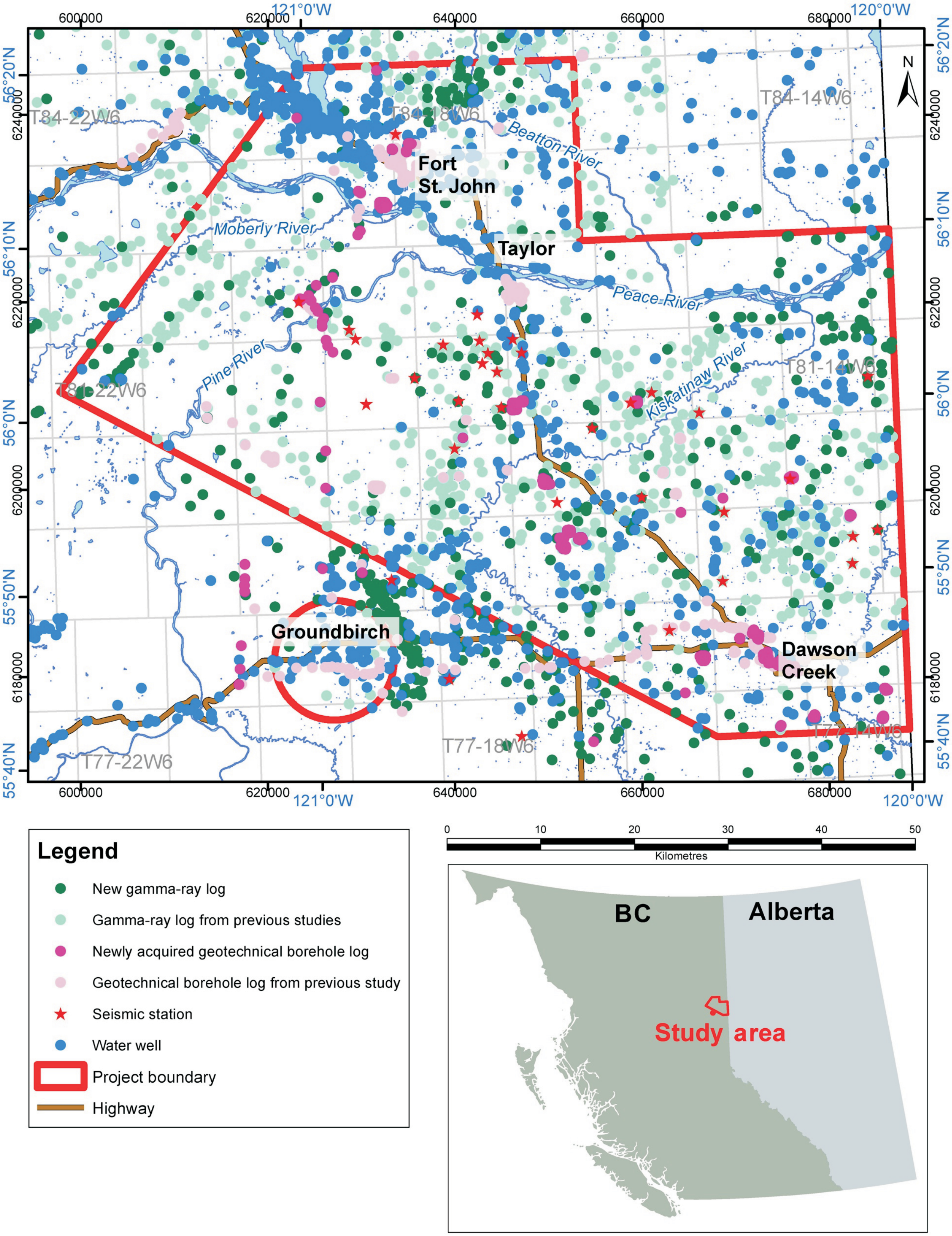

Figure 1. Map of the study area showing the location of subsurface geological database sites. Previous studies are those by Petrel Robertson Consulting Ltd. (2016; gamma-ray logs) and Monahan et al. (2019; gamma-ray logs, geotechnical borehole logs). All co-ordinates are in UTM Zone 10N, NAD83.

ciofluvial sand and gravel representing the earliest phases of postglacial fluvial incision. Modern fluvial sand and gravel occupy river valley bottoms.

Within the upland areas, the valleys of minor streams have gently sloping floors and are underlain by glaciolacustrine sediments, into which the modern streams have now incised. The degree of incision increases markedly as these streams approach the major valleys. Boundaries between the upland areas and adjacent glaciolacustrine terraces, platforms and valley bottoms are commonly marked by distinct breaks in slope. However, these breaks in slope are not as clear in the areas of subdued topography in the east.

Surficial Geology Mapping

Detailed topographic mapping at a 5 m contour interval and slope mapping have been computed from a Natural Resources Canada digital elevation model (Natural Resources Canada, 2015). These enable more reliable definition of the breaks in slope that mark the boundaries of the glaciolacustrine platforms with the adjoining uplands and with the deeply incised river valleys than shown on existing surficial geological maps (Mathews, 1978; Reimchen, 1980).

An eight-day field program was also conducted in August 2019 to spot check the interpretations, observe landforms and note the topographic setting of sites with subsurface geological data and seismograph stations established by government and industry to monitor induced seismic activity.

Subsurface Geological Database

As with the previous study, three sources of subsurface geological data are being employed: cased-hole gamma-ray logs from petroleum wells, water well logs and geotechnical borehole logs.

Gamma-ray logs run through surface casing to (near) surface are required for petroleum well sites drilled in BC and are available in public databases. Top of bedrock can be picked with reasonable confidence where stratigraphic markers in Cretaceous strata are truncated and overlain by Quaternary sediments, particularly where bedrock consists of marine shale, in which abundant markers can be traced over tens of kilometres (Hayes et al., 2016; Petrel Robertson Consulting Ltd., 2016; Monahan et al., 2019). For the studies by Petrel Robertson Consulting Ltd. (2016) and Monahan et al. (2019), logs from 918 wells in and adjacent to the project area were normalized to remove surface casing effects (documented by Quartero et al., 2014). These data are being used for the current study. An additional 458 gamma-ray logs, which represent all those remaining in the area, have been added to this dataset (Figure 1). Even though gamma-ray log data are highly repeatable, each log curve provides only limited lithological information. Furthermore, not all logs have been run continuously to surface and, in many places, attenuation of the gamma-ray signal by the conductor pipe obscures the lithological signature in the upper 10 to 30 m. Where the bedrock top is shallow and lies above the top of the logged interval, all that can be reported is a maximum depth to bedrock. Nonetheless, cased-hole gamma-ray logs provide important constraints on thickness and lithology of the Quaternary section, particularly when combined with other subsurface geological data.

An edited database of depth to bedrock values in northeastern BC water wells was prepared by Hickin (2013), primarily from the BC Ministry of Environment and Climate Change Strategy's GWELLS database (https://apps.nrs.gov.bc.ca/gwells/). This dataset has been updated from those used in previous studies, and includes 1282 wells in and adjacent to the project area (Figure 1). Although it includes an enormous amount of useful information, it has been generated from water well records prepared with large variations in accuracy of lithological descriptions and unit depths, and well locations are in some cases suspect.

Geotechnical borehole logs provide the best data for Quaternary geological studies, because they are consistently described by professionals, reliably located and include repeatable quantitative measurements that can be correlated to physical properties. The latter include standard penetration test (SPT) blowcount (N) values and moisture content, which are useful stratigraphic indices. The SPT N value is the number of hammer blows required to drive a sample tube 305 mm (1 ft.) into the material at the bottom of the hole under standardized conditions. If after 50 blows, penetration has not reached 305 mm, the test is usually terminated; this upper limit is termed refusal, and indicates a material very resistant to penetration. The principal disadvantage of these borehole data is that they are generally drilled to very shallow depths, a few tens of metres at most. Furthermore, they are proprietary and so laborious to compile. Monahan et al. (2019) obtained 582 borehole logs at 107 sites in and adjacent to the current project area and these are being used in the current study. To supplement these, an additional 592 borehole logs at 99 sites have been obtained to date, and data collection is ongoing (Figure 1). Of the 206 sites represented, 143 have data deeper than 10 m.

Acquisition of V_S Data and Initial Results

New V_S data have been obtained by downhole logging using the vertical seismic profiling (VSP) method, and by multichannel analysis of surface waves (MASW), a non-invasive surface technique that generates a V_S profile along a 100 m transect. These two methods are described by Arsenault et al. (2012) and Phillips and Sol (2012), respectively.

Monahan et al. (2019) acquired V_S data at 14 sites in and adjacent to the project area (Figure 2). These included six

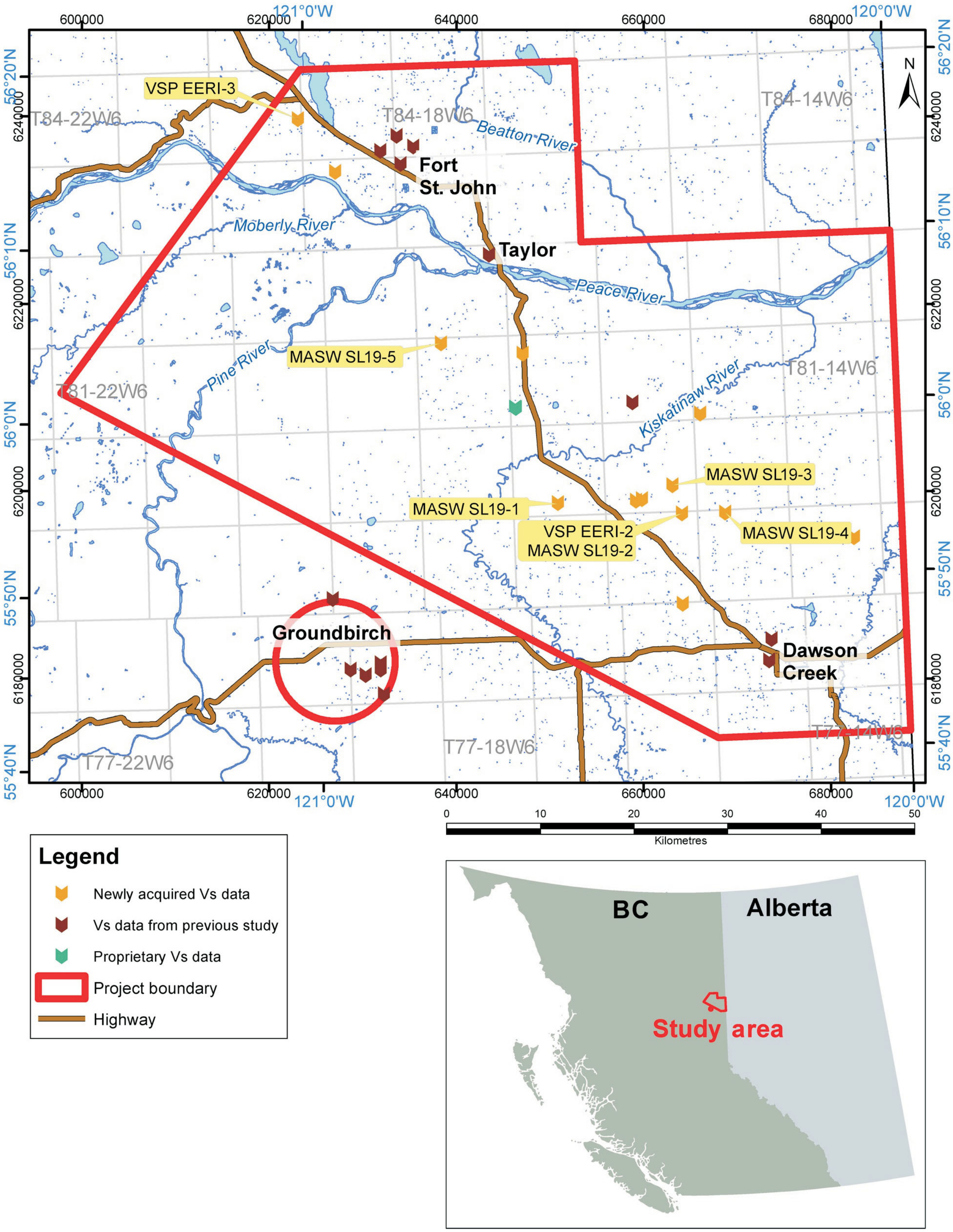

Figure 2. Spatial distribution of shear-wave velocity (V_S) data. Sites identified are those shown in Table 2. Previous study is that by Monahan et al. (2019). All co-ordinates are in UTM Zone 10N, NAD83. Abbreviations: MASW, multichannel analysis of surface waves; VSP, vertical seismic profiling.

downhole logs in pre-existing cased boreholes acquired by the VSP method at Groundbirch, south of the project area, and eight MASW profiles. The latter were concentrated in a few areas – four in Fort St John, two in Dawson Creek, one at Taylor, and only one in the rural areas south of the Peace River, which constitute most of the current project area.

To date, an additional four downhole logs in pre-existing boreholes and 10 new MASW profiles have been acquired (Figure 2). Two of the boreholes were drilled by the Energy and Environment Research Initiative (EERI) as part of a regional groundwater monitoring project by The University of British Columbia (Cahill et al., 2019), and the other two are Province of BC groundwater observation wells. In addition to V_S data, P-wave velocity (V_P) and gamma-ray data were acquired. Most of the MASW tests were done at seismograph stations, in order to correct seismic records for site effects and to understand the seismic responses at these stations. An additional two downhole logs in existing boreholes and 10 to 12 MASW tests are being planned. Proprietary V_S data have also been obtained at one site.

At the time of writing, V_S data have been received for the first two boreholes, EERI-2 and-3 (Figures 3, 4), and the first five MASW tests (Figures 5–7). The results are summarized in Table 2. To estimate the site period, the depth of the low-velocity surface layer was determined from the most abrupt V_S change on the downhole logs, and the main inflection below the surface layer on the MASW profiles, at the profile midpoint. Stations MONT 1 (MASW SL19-1) and MONT 8 (MASW SL19-5) are part of a network established by the BC Oil and Gas Commission and Natural Resources Canada, and station MG05 (MASW SL19-4) is part of a network established for the McGill University Dawson-Septimus induced seismicity study. An MASW test was conducted adjacent to borehole EERI-2 (MASW SL19-2) to compare the results of the two techniques.

Some observations can be made, and conclusions drawn, from the new data. All the new V_S sites are in Site Class D, with V_{S30} ranging from 228 to 345 m/s. These sites occupy a range of geomorphic settings, from a valley bottom site, where the low velocity layer corresponds to glaciolacustrine clay (MASW SL19-1; Figures 2, 5, Table 2) and Site

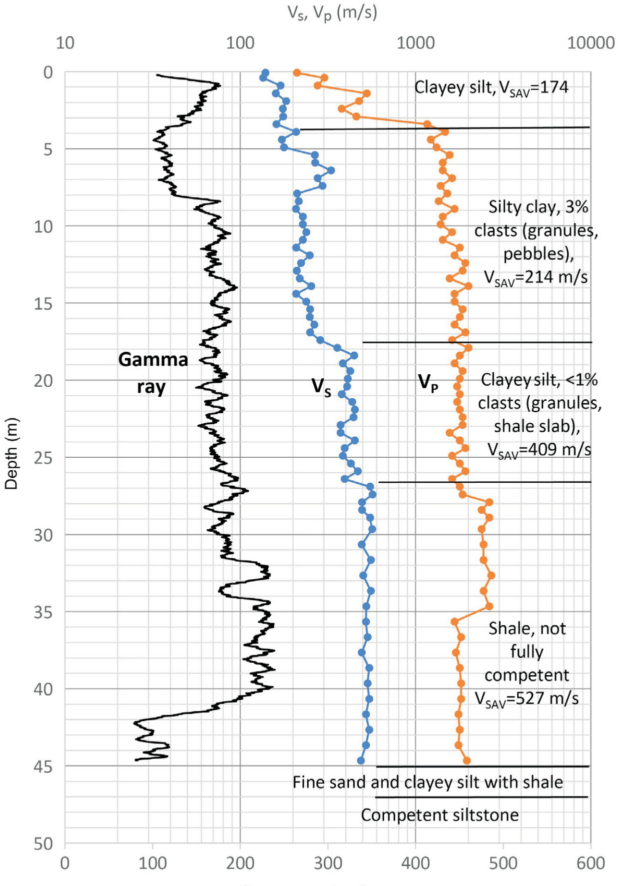

Figure 3. Borehole log for EERI-2. Gamma-ray, shear-wave velocity (V_S) and P-wave velocity (V_P) data. Lithological log and descriptions adapted from that of M. Goetz (Cahill et al., 2019). Note gamma-ray scale at bottom. Abbreviations: cps, counts per second; V_{SAV}, interval average of shear-wave velocity.

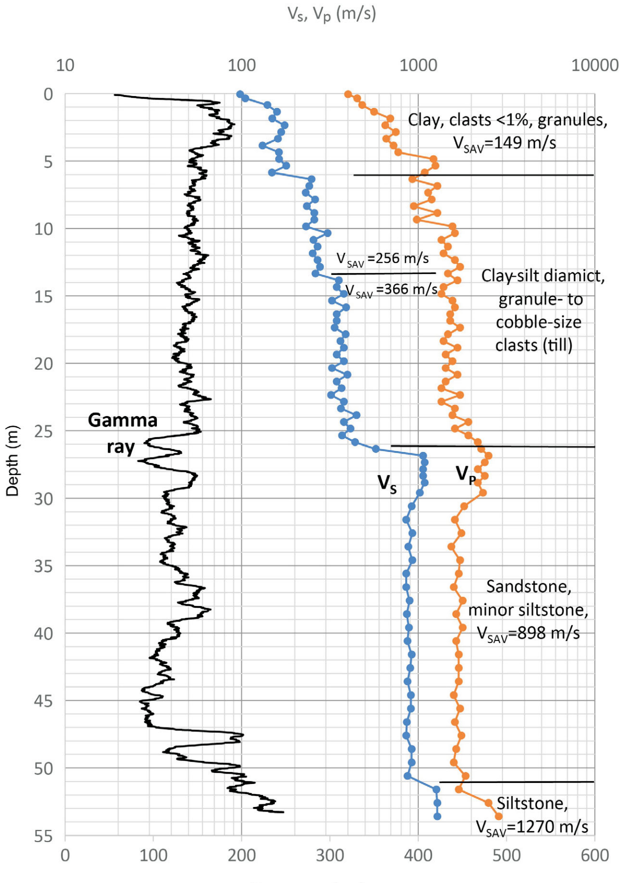

Figure 4. Borehole log for EERI-3. Gamma-ray, shear-wave velocity (V_S) and P-wave velocity (V_P) data. Lithological log and descriptions adapted from that of M. Goetz (Cahill et al., 2019). Note gamma-ray scale at bottom. Abbreviations: cps, counts per second; V_{SAV}, interval average of shear-wave velocity.

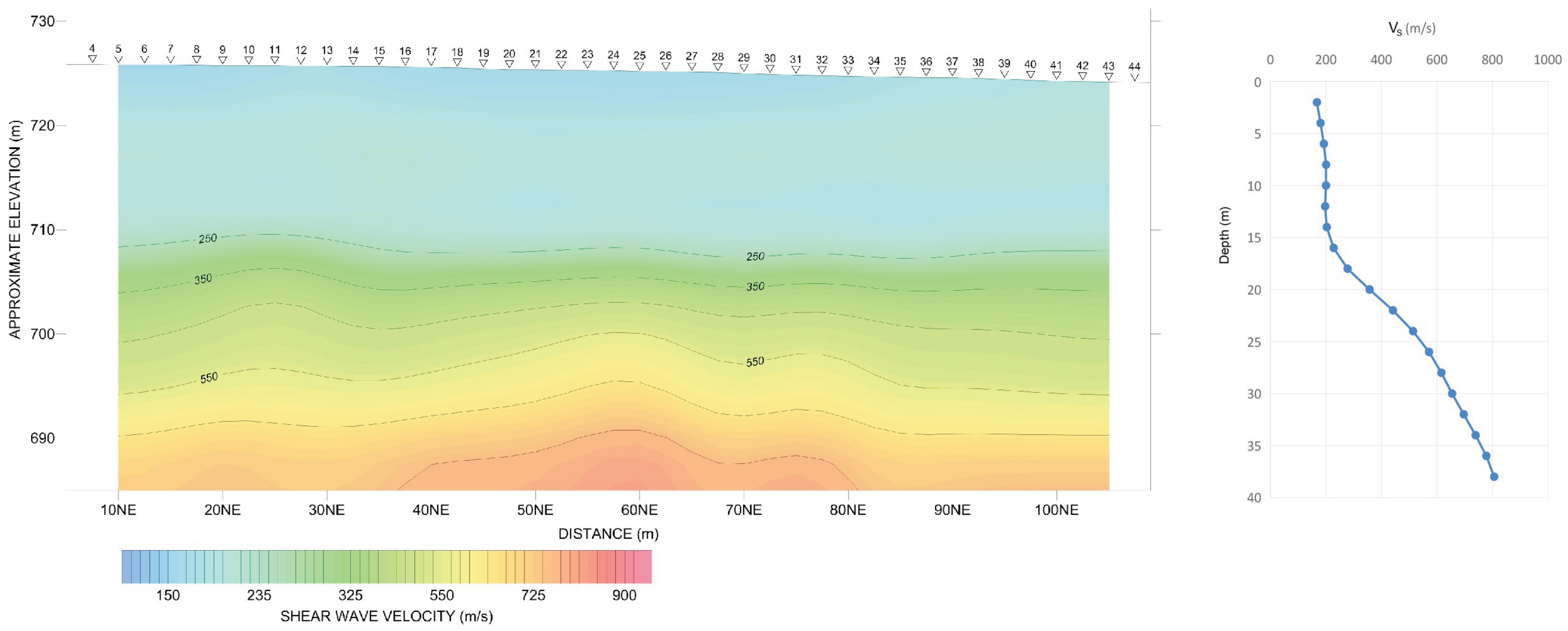

Figure 5. Multichannel analysis of surface waves at MASW SL19-1 (station MONT 1), valley bottom location; left panel, profile; right panel, shear-wave velocity (V_S) trace in middle of profile. Numbers along the top of the profile are geophone locations. Abbreviation: NE, to the northeast.

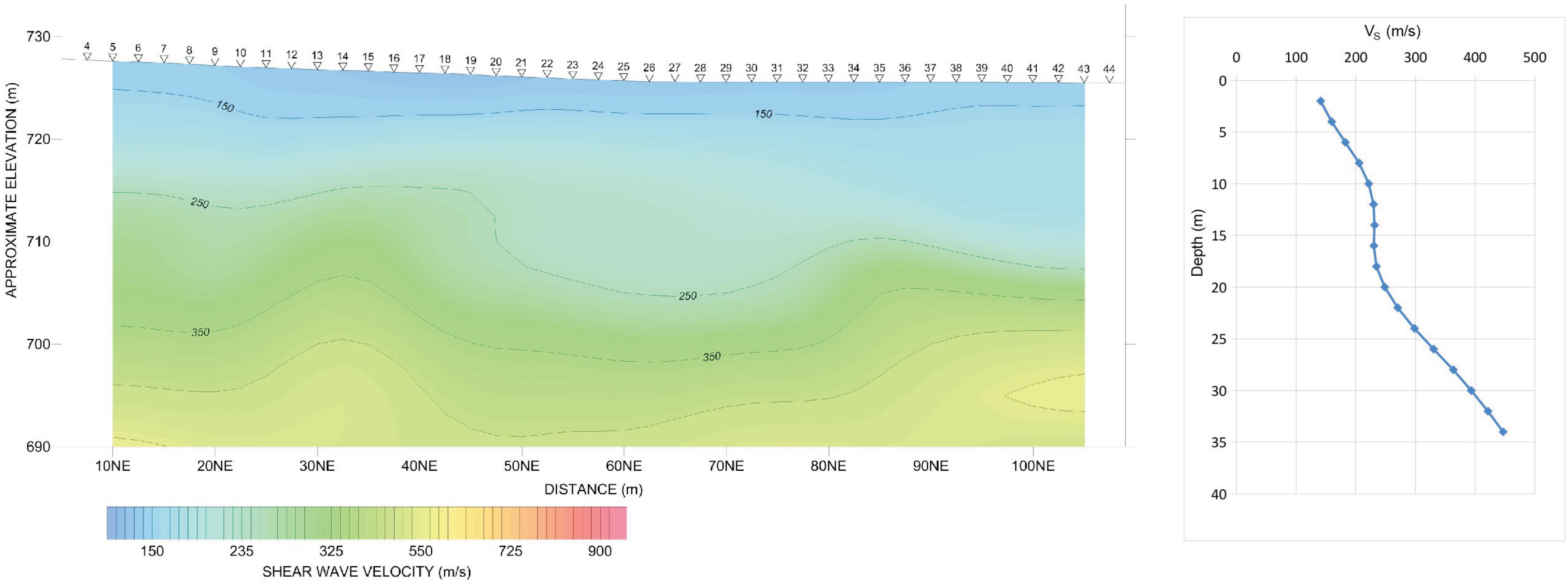

Figure 6. Multichannel analysis of surface waves at MASW SL19-2, adjacent to the site of borehole EERI-2 (Figure 3), on gently sloping hillside; left panel, profile; right panel, shear-wave velocity (V_S) trace in middle of profile. Numbers along the top of the profile are geophone locations. Abbreviation: NE, to the northeast.

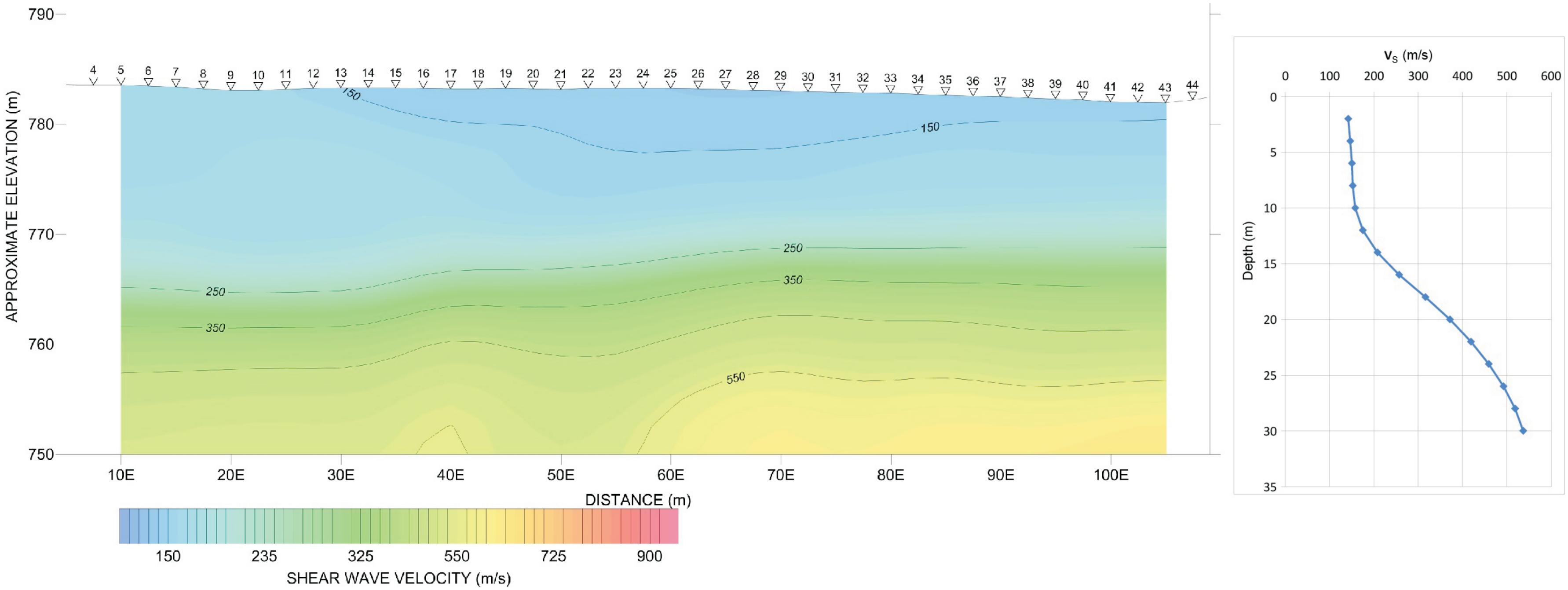

Figure 7. Multichannel analysis of surface waves at MASW SL19-4 (station MG05) at 16-32-79-15W6 (L.S. 16, Sec. 32, Twp. 79, Rge. 15, W 6th Mer.) well site, on a hilltop; left panel, profile; right panel, shear-wave velocity (V_S) trace in middle of profile. Numbers along the top of the profile are geophone locations. Abbreviation: E, to the east.

Table 2. Summary of new shear-wave velocity (V_S) data acquisition and results. These test sites are identified on Figure 2. All co-ordinates are in UTM Zone 10N, NAD83.

Number	Location/ borehole/ station number	Easting (m)	Northing (m)	Depth (m)	V_{S30} (m/s)	Site Class	Low velocity layer Thickness (m)	Low velocity layer V_{SAV} (m/s)	Site period (s)	Setting
VSP EERI-2	EERI-2	664116	6197620	45	270	D	17.7	214	0.33	Gently sloping hillside
VSP EERI-3	EERI-3	623071	6239713	55	278	D	26.1	250	0.42	Minor valley bottom in hilly terrain
MASW SL19-1	Station MONT 1	650843	6198718	38	253 ±4	D	15	189	0.31	Valley bottom, 7 m clay in dugout
MASW SL19-2	EERI-2	664116	6197620	34	228 ±7	D	19	194	0.39	Gently sloping hillside
MASW SL19-3	Industry station 11-11-80-16W6[1]	663081	6200617	36	345 ±14	D	13	280	0.19	Steep hillside
MASW SL19-4	Station MG05, 16-32-79-15W6	668703	6197693	30	233 ±13	D	12	151	0.32	Hilltop
MASW SL19-5	Station MONT 8	638356	6215783	36	246 ±16	D	19	189	0.40	Gently sloping hillside

[1] L.S. 11, Sec. 11, Twp. 80, Rge. 16, W 6th Mer.

Class D is expected, to upland sites, where surficial deposits are primarily till and Site Class C had been previously assigned (Monahan et al., 2019). These data demonstrate that the low blowcount (N=15 to 50) till recognized in many of the geotechnical boreholes obtained for this study is characterized by low V_S (150–300 m/s), and that in the upland areas where topography is more subdued in the central and eastern parts of the study area, geotechnical borehole data show that till forms a blanket 10 to 30 m thick. An example is the hilltop MASW site (MASW SL19-4; Figures 2, 7, Table 2), where the low velocity layer correlates with till in a nearby borehole (M. Goetz and B. Ladd, pers. comm., 2019). Consequently, Site Class D occurs commonly within the upland hillsides and hilltops.

However, Site Class C conditions have also been documented in upland areas, both where bedrock is shallow (<7 m), and where the till section is dominated by high-blowcount (N>50) and high-V_S (>400 m/s) intervals (Monahan et al., 2019). These intervals generally occur stratigraphically below low-blowcount, low-V_S till. An example of the latter is provided by the VSP log from EERI-3, where V_S in the till interval increases abruptly from 256 to 366 m/s at 13.5 m (Figure 4). The V_S increase does not reflect a change in lithology (Cahill et al., 2019), but increased glacial compaction. In this case, the thickness of low-V_S till keeps this site in Site Class D. Consequently, Site classes C and D both occur in upland areas, and further integration of the borehole, V_S and topographic data will be necessary to determine areas dominated by each Site Class. In addition, the authors acknowledge that blowcount data in till must be interpreted carefully, as high blowcounts can also occur in low-V_S till where the SPT is performed directly on a large clast.

The V_{S30} calculated from the MASW test (MASW SL19-2) conducted adjacent to borehole EERI-2 is 228 m/s, which is significantly lower than that in the VSP log for EERI-2, V_{S30} of 270 m/s (Table 2, Figures 2, 3, 6). This discrepancy will be investigated further. However, the V_S of bedrock above 47 m in the VSP log is 527 m/s, which is low compared to other bedrock intervals (Monahan et al., 2019), and it is described as not fully competent and is underlain by beds of silt and fine sand (Cahill et al., 2019; Monahan et al., 2019). This suggests it may be a glaciotectonized or glacially transported block in which extensive fracturing has reduced the V_S relative to undisturbed bedrock. Consistent with this, V_S in the lower part of the MASW profile is variable, suggesting a disrupted stratigraphic succession. The larger volume of material investigated by MASW may include a larger number of Quaternary interbeds and fractures, resulting in lower V_S than in the VSP log.

Interviews with Residents

Residents at 12 households, ranging from near Dawson Creek to the Pine River, have been interviewed to date to record their experiences with induced earthquakes. A common experience is hearing a loud thump or rumbling, like a train, truck or cow coming through the house, loud enough to wake people at night. Others describe rattling of windows and dishes. These observations are consistent with modified Mercalli intensity IV. The differences in experiences may correlate with differences in geological and topographic setting. Some residents report several events in a single day during ongoing hydraulic fracturing operations. Acquisition of MASW profiles is planned to determine the V_{S30} and V_S structure at five of these residences and additional interviews will be conducted.

Conclusions

The initial results of this project demonstrate that Site Class D conditions are widespread. They occur not only in areas underlain by glaciolacustrine silt and clay, as previously recognized, but also in the upland slopes and hilltops, where Site Class C had been assigned previously. This is due to the common occurrence of low–shear-wave velocity till, locally up to 30 m thick.

Further integration of subsurface geological datasets with shear-wave velocity and topographic data is required to determine which areas are dominated by Site Class D rather than Site Class C conditions. These will be compared with instrumental earthquake records and residents' reports to determine where induced seismic events are more strongly felt.

Acknowledgments

The authors gratefully thank the following organizations and individuals:

- Geoscience BC for providing project funding;
- for assistance in acquiring geotechnical borehole data: Northern Geo Testing and Engineering; Urban Systems; City of Fort St. John; City of Dawson Creek; District of Taylor; Peace River Regional District; School Board 60: Peace River North; BC Hydro; BC Oil and Gas Commission; Shell Canada Limited; ARC Resources Ltd; Crew Energy Inc.; Encana Corporation; Canadian Natural Resources Ltd.; and The University of British Columbia's (UBC) Energy and Environment Research Initiative (EERI) Program; particular thanks to B. Rodowski, B. Ladd and J. Cegnar;
- for access to field sites: UBC EERI Program, BC Ministry of Forests, Lands, Natural Resource Operations and Rural Development, McGill University Dawson-Septimus induced seismicity project, BC Oil and Gas Commission, Tourmaline Oil Corp., Northern Lights College, ARC Resources Ltd., Crew Energy Inc., Canadian Natural Resources Ltd., Encana Corporation, Shell Canada Limited; particular thanks to L. Hurrell, M. Goetz, G. Langston, A. Babaie Mahani, K. Evers, R. Nakamoto, D. McHarg and several residents who granted access to their lands;
- for helpful discussions: S. Venables, J. Johnson, A.S. Hickin and A. Babaie Mahani;
- K. Hadavi and J. Cegnar of BC Hydro for arranging a tour of Site C;
- L. Sears for assembling the manuscript;
- an anonymous reviewer for reviewing the manuscript and suggesting many helpful changes;
- and to several residents of the region for providing information and detailed accounts of their experiences.

References

Arsenault, J.-L., Hunter, J.A. and Crow, H.L. (2012): Shear wave velocity logs from vertical seismic profiles; *in* Shear Wave Velocity Measurement Guidelines for Canadian Seismic Site Characterization in Soil and Rock, J.A. Hunter and H.L. Crow (ed.), Geological Survey of Canada, Open File 7078, p. 123–138.

Atkinson, G.M., Eaton, D.W., Ghofrani, H., Walker, D., Cheadle, B., Schultz, R., Shcherbakov, R., Tiampo, K., Gu, J., Harrington, R.M., Liu, Y., van der Baan, M. and Kao, H. (2016): Hydraulic fracturing and seismicity in the Western Canada Sedimentary Basin; Seismological Research Letters, v. 87, no. 3, p. 1–17.

Babaie Mahani, A. and Kao, H. (2018): Ground motion from M 1.5 to 3.8 induced earthquakes at hypocentral distance <45 km in the Montney play of northeast British Columbia, Canada; Seismological Research Letters, v. 89, no. 1, p. 22–34.

Babaie Mahani, A., Kao, H., Atkinson, G.M., Assatourians, K., Addo, K. and Liu, Y. (2019): Ground-motion characteristics of the 30 November 2018 injection-induced earthquake sequence in northeast British Columbia, Canada; Seismological Research Letters, v. 90, no. 4, p. 1457–1467, URL <https://doi.org/10.1785/0220190040> [July 2019].

Babaie Mahani, A., Kao, H., Johnson, J. and Salas, C. (2017a): Ground motion from the August 17, 2015, moment magnitude 4.6 earthquake induced by hydraulic fracturing in northeastern British Columbia; *in* Geoscience BC Summary of Activities 2016, Geoscience BC, Report 2017-01, p. 9–14, URL <http://www.geosciencebc.com/i/pdf/SummaryofActivities2016/SoA2016_BabaieMahani.pdf> [October 2017].

Babaie Mahani, A., Schultz, R., Kao, H., Walker, D., Johnson, J. and Salas, C. (2017b): Fluid injection and seismic activity in the northern Montney Play, British Columbia, Canada, with special reference to the 17 August 2015 Mw 4.6 induced earthquake; Bulletin of the Seismological Society of America, v. 107, p. 542–552.

Building Seismic Safety Council (2003): NEHRP recommended provisions for seismic regulations for new buildings and other structures (FEMA 450), part 1: provisions (2003 edition); prepared for the Federal Emergency Management Agency, 338 p., URL <http://www.nehrp.gov/pdf/fema450provisions.pdf> [October 2017].

Cahill, A.G., Beckie, R.D., Goetz, M., Allen, A., Ladd, B., Welch, L., Kirste, D., Mayer, B. and van Geloven, C. (2019): Characterizing dissolved methane in groundwater in the Peace region, northeastern British Columbia, using a regional, dedicated, groundwater monitoring well network; *in* Geoscience BC Summary of Activities 2018: Energy and Water, Geoscience BC, Report 2019-02, p. 105–122, URL <http://cdn.geosciencebc.com/pdf/SummaryofActivities2018/EW/2017-002_SoA2018_EW_Cahill_DissolvedMethane.pdf> [November 2019].

Finn, W.D.L. and Wightman, A. (2003): Ground motion amplification factors for the proposed 2005 edition of the National

Building Code of Canada; Canadian Journal of Civil Engineering, v. 30, p. 272–278.

Hartman, G.M.D. and Clague, J.J. (2008): Quaternary stratigraphy and glacial history of the Peace River valley, northeast British Columbia; Canadian Journal of Earth Sciences, v. 45, p. 549–564.

Hartman, G.M.D., Clague, J.J., Barendregt, R.W. and Reyes, A.V. (2018): Late Wisconsinan Cordilleran and Laurentide glaciation of the Peace River Valley east of the Rocky Mountains, British Columbia; Canadian Journal of Earth Sciences, v. 55, no. 12, p. 1324–1338.

Hayes, B.J.R., Levson, V., Carey, J. and Mykula, Y. (2016): Interpretation of Quaternary sediments and depth to bedrock, Peace Project area, northeastern British Columbia: project update; *in* Geoscience BC Summary of Activities 2015, Geoscience BC, Report 2016-01, p. 61–68, URL <http://www.geosciencebc.com/i/pdf/SummaryofActivities2015/SoA2015_Hayes.pdf> [October 2017].

Hickin, A.S. (2013): Late Quaternary to Holocene geology, geomorphology and glacial history of Dawson Creek and surrounding area, northeast British Columbia, Canada; Ph.D. thesis, University of Victoria, 369 p.

Hickin, A.S., Best, M.E. and Pugin, A. (2016a): Geometry and valley-fill stratigraphic framework for aquifers in the Groundbirch paleovalley assessed through shallow seismic and ground-based electromagnetic surveys; BC Ministry of Energy, Mines and Petroleum Resources, BC Geological Survey, Open File 2016-5, 46 p.

Hickin, A.S., Lian, O.B. and Levson, V.M. (2016b): Coalescence of late Wisconsinan Cordilleran and Laurentide ice sheets east of the Rocky Mountain Foothills in the Dawson Creek region, northeast British Columbia, Canada; Quaternary Research, v. 85, p. 409–429.

Hickin, A.S., Lian, O.B., Levson, V.M. and Cui, Y. (2015): Pattern and chronology of glacial Lake Peace shorelines and implications for isostasy and ice-sheet configuration in northeastern British Columbia, Canada; Boreas, v. 44, p. 288–304.

Holland, S.S. (1976): Landforms of British Columbia – a physiographic outline (second edition); BC Ministry of Energy, Mines and Petroleum Resources, Bulletin 48, 138 p.

Hollingshead, S. and Watts, B.D. (1994): Preliminary seismic microzonation assessment for British Columbia; prepared for Resources Inventory Committee, Earth Sciences Task Force, 109 p.

Irish, E.J.W. (1958): Charlie Lake, West of Sixth Meridian, British Columbia; Geological Survey of Canada, Preliminary Map 17-1958, scale 1:253 440, 1 sheet.

Kao, H., Hyndman, R., Jiang, Y., Visser, R., Smith, B., Babaie Mahani, A., Leonard, L., Ghofrani, H. and He, J. (2018): Induced seismicity in western Canada linked to tectonic strain rate: implications for regional seismic hazard; Geophysical Research Letters, v. 45, 12 p., URL <https://doi.org/10.1029/2018GL079288> [November 2018].

Kramer, S.L. (1996): Geotechnical Earthquake Engineering; Prentice-Hall, Inc., Upper Saddle River, New Jersey, 653 p.

Mathews, W.H. (1978): Quaternary stratigraphy and geomorphology of the Charlie Lake (94A) map-area, British Columbia; Geological Survey of Canada, Paper 76-20, 25 p., includes Map 1460A, scale 1:250 000.

Mathews, W.H. (1980): Retreat of the last ice sheets in northeastern British Columbia and adjacent Alberta; Geological Survey of Canada, Bulletin 331, 22 p.

McMechan, M.E. (1994): Geology and structure cross section, Dawson Creek, British Columbia; Geological Survey of Canada, Map 1858A, scale 1:250 000.

Monahan, P.A., Levson, V.M., Hayes, B.J., Dorey, K., Mykula, Y., Brenner, R., Clarke, J., Galambos, B., Candy, C., Krumbiegel, C. and Calderwood, E. (2019): Mapping the susceptibility to amplification of seismic ground motions in the Montney play area of northeastern British Columbia; Geoscience BC Report 2018-16, 65 p., URL <http://cdn.geosciencebc.com/project_data/GBCR2018-16/GBCR2018-16-NEBC_Amplification_Report.pdf> [November 2019].

National Research Council (2015): National Building Code of Canada; National Research Council, Ottawa, v. 1, 708 p.

Natural Resources Canada (2015): Canadian Digital Elevation Model; Natural Resources Canada, URL <https://open.canada.ca/data/en/dataset/7f245e4d-76c2-4caa-951a-45d1d2051333> [May 2019].

Petrel Robertson Consulting Ltd. (2016): Interpretation of Quaternary sediments and depth to bedrock, Peace Project area, northeastern British Columbia; Geoscience BC, Report 2016-04, URL <http://www.geosciencebc.com/reports/gbcr-2016-04/> [October 2017].

Phillips, C. and Sol, S. (2012): Multichannel analysis of surface waves (MASW) technique for hazard studies; *in* Shear Wave Velocity Measurement Guidelines for Canadian Seismic Site Characterization in Soil and Rock, J.A. Hunter and H.L. Crow (ed.), Geological Survey of Canada, Open File 7078, p. 62–66.

Quartero, E.M., Bechtel, D., Leier, A.J. and Bentley, L.R. (2014): Gamma-ray normalization of shallow well-log data with applications to the Paleocene Paskapoo Formation, Alberta; Canadian Journal of Earth Sciences, v. 51, p. 452–465.

Reimchen, T.H.F. (1980): Surficial geology, Dawson Creek, West of the Sixth Meridian, British Columbia; Geological Survey of Canada, Map 1467A, scale 1:250 000.

Stott, D.F. (1982): Lower Cretaceous Fort St. John Group and Upper Cretaceous Dunvegan Formation of the foothills and plains of Alberta, British Columbia, and District of Mackenzie and Yukon Territory; Geological Survey of Canada, Bulletin 328, 124 p.

Worden, C.B., Gerstenberger, M.C., Rhoades, D.A. and Wald, D.J. (2012): Probabilistic relationships between ground-motion parameters and modified Mercalli intensity in California; Bulletin of the Seismological Society of America, v. 102, p. 204–221.